Performance of Nanocrystalline Iron Pyrite as the Back Contact to CdS/CdTe Solar Cells

Khagendra P. Bhandari, Rajendra R. Khanal, Naba R. Paudel, Prakash Koirala, Paul J. Roland, Tyler Kinner, Yanfa Yan, Robert W. Collins, Michael J. Heben, and Randy. J. Ellingson

Wright Center for Photovoltaic Innovation and Commercialization, Department of Physics and Astronomy, The University of Toledo, 2801 W. Bancroft Street, Toledo, OH 43606

***Abstract* — We describe the application of iron persulfide (pyrite, FeS_2) NC thin films as a Cu-free back contact to CdS/CdTe solar cells. We synthesized cubic FeS_2 NCs, and prepared NC-FeS_2 films by drop-casting to investigate their use in thin film solar cells. Characterization of the FeS_2 NC films revealed sub-band-gap optical absorption, holes as the majority carrier, free hole concentration of ~10^{19} cm^{-3}, and Hall mobility of $\mu_h << 1$ cm^2 $V^{-1}S^{-1}$. CdS/CdTe solar cells completed by depositing hydrazine-treated NC-FeS_2 back contacts directly onto CdTe displayed efficiencies comparable to those of standard Cu/Au back contact devices. Our best FeS_2 device shows an AM1.5G efficiency of 12.5%, V_{oc} = 0.81 V, J_{sc} = 23.0 mA/cm^2, and FF = 67%. Temperature dependent studies of solar cells reveal that the 'roll-over' effect observed in standard devices at low temperature is controlled by replacing Cu by hydrazine-treated NC-FeS_2.**

***Index Terms* – back contact, cadmium telluride, hydrazine, iron persulfide, iron pyrite, nanocrystal, copper-free, carrier density, mobility**

I. INTRODUCTION

Starting in the 1980's, iron persulfide (pyrite, FeS_2) has attracted considerable attention as a potential light-absorbing layer in thin film solar cells because of its high absorption coefficient and suitable band gap energy.[1-3] Despite a relative lack of early success with FeS_2 solar cells, interest has recently increased in studying the synthesis and application of iron pyrite in photovoltaic devices. Following Tributsch et al.'s 2.8% efficient photochemical device [1], Kirkeminde et al. has demonstrated a 1.1% efficient solar cell incorporating NC FeS_2 within a polymer matrix to produce a CdS-QD/hybrid device.[4] Here, we discuss the properties of FeS_2 NCs and NC thin films, and describe their use as a Cu-free back contact to CdS/CdTe solar cells. Although use of Cu within the back contact to CdTe is commonplace, concerns remain regarding the stability of Cu within the CdS/CdTe device structure. Copper diffusion is understood to degrade the long term performance of the devices by producing junction-shunting pathways.[5, 6] Development of a stable and efficient back contact, free of Cu, may favorably influence the economics of the CdTe technology platform. Our preliminary results show that FeS_2 serves as an effective low-barrier back contact for CdS/CdTe solar cells.

Charge carrier transport in semiconductors is greatly influenced by the temperature. Temperature dependent current-voltage characteristics of a device help to understand the behavior of thermally generated charge carrier mobility and mechanism of photocurrent and photovoltage generations in the devices. In this paper, we have also included preliminary temperature dependent J-V characteristics of CdS/CdTe solar cells employing either standard Cu/Au or NC-FeS_2/Au as back contacts.

II. EXPERIMENTAL METHODS

A. Iron pyrite (FeS_2) synthesis

Iron pyrite NCs were synthesized via a solution-based method using iron (II) bromide as the iron precursor, elemental sulfur as a sulfur source, trioctylphosphine oxide (TOPO) or 1,2-hexanediol as coordinating solvents, and oleylamine (OLA) as a non-coordinating solvent. The synthesis was accomplished in a Schlenck line using nitrogen for the inert atmosphere.

B. Iron pyrite NC solution and film characterization

For the complete identification of these NCs, several experimental methods including UV/Vis/NIR spectroscopy, XRD spectroscopy, Raman spectroscopy, SEM and EDX were used. We characterized FeS_2 NC samples both as solution suspensions in chloroform as well as in thin film form. Thin films were prepared using drop-casting onto substrates of interest. For FeS_2 film characterization, zero back ground single crystalline silicon and soda-lime glass were used as substrates. Electrical properties of these NC-based thin films were studied using four point probe, Hall measurement and hot probe measurements. For device fabrication, CdS/CdTe deposited devices were used as substrates for FeS_2 film fabrication. FeS_2 NC films were deposited at room temperature using a layer by layer (LbL) drop-cast method. In the LbL process, FeS_2 NC films were dipped into 1 M hydrazine in ethanol to remove surfactant molecules from the surface of the NCs.

C. Iron pyrite NC film as a back contact

To test FeS_2 NC thin films as back contact, devices fabricated by either RF magnetron sputtering or close spaced sublimation (CSS) methods were used. For comparison

purposes, CdTe devices with back contacts of Au and Cu/Au were also fabricated; devices with Cu/Au back contact were considered as standard devices. The thicknesses of sputtered and CSS-deposited CdTe were ~2 μm and ~4 μm, respectively, whereas the thickness of CdS was ~80 nm in both cases. Before the back contact deposition, $CdCl_2$ treatment was utilized to promote grain growth, reduced defect density, reduce interfacial strain, and facilitate sulfur and tellurium mixing at the interface. [7]

III. EXPERIMENTAL RESULTS AND DISCUSSION

A. Characterizations of FeS_2 NCs

Fig. 1(a) depicts the absorbance spectra of FeS_2 NCs dispersed in chloroform. Absorbance spectra indicate that most of the light absorption takes place in visible and near infrared regions of the spectrum. Using absorption spectra of NC films, we were able to calculate the direct band gap to be 1.3 eV and the indirect band gap to be 0.95 eV. The sub-band-gap optical absorption in FeS_2 NCs may be due to the defects states or structural disorder. However, Lazic et al. recently reported that their density functional theory model indicates a smaller band gap for FeS_2 than recently in use in the literature[8], and this may explain the absorption beyond ~1.3 μm..

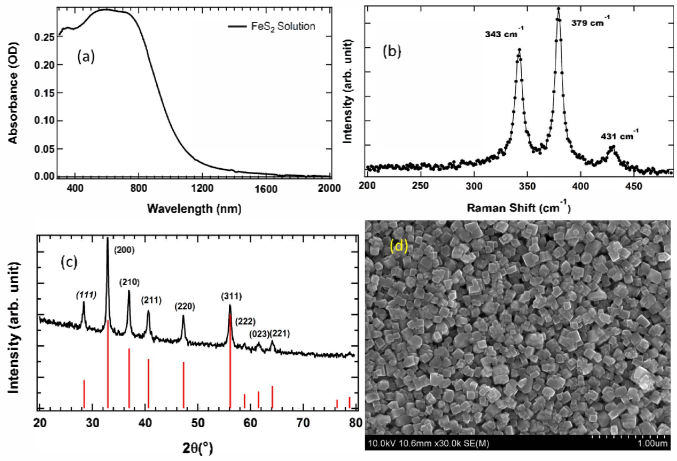

Fig. 1. (a) Absorbance spectra of as-obtained FeS_2 NCs of size ~70 nm dispersed in chloroform, (b) Raman spectrum, (c), XRD pattern with iron pyrite standard, and (d) SEM micrograph of a drop-cast film of as-synthesized TOPO-capped FeS_2 NCs of size ~130 nm.

The Raman spectrum in Fig. 1(b) shows peaks at 343 cm^{-1}, 379 cm^{-1} and 431 cm^{-1} consistent with the phonon vibration of FeS_2 and matching the literature values [9-11]. The XRD image in Fig. 1(c) shows a pure cubic phase of FeS_2 with no other phases evident. Thin film XRD data were collected using Cu Kα radiation in focused beam geometry. XRD data show excellent crystallinity of the as-obtained FeS_2 NCs. In Fig. 1(c), vertical lines represent peak positions for standard FeS_2 pyrite phase annotated with Miller indices. The cubic shape of these NCs can be seen in SEM image as shown in Fig. 1(d). FeS_2 NCs of various sizes, ranging from 70 nm to 130 nm, were synthesized in separate batches. EDX measurement of samples from seven different syntheses shows that the S:Fe ratio is 2.01:1, representing a nearly-stoichiometric compound.

To reduce the propensity for pinholes within FeS_2 NC thin films, our NC films were prepared using a LbL method alternating between drop-casting and hydrazine treatment. Hydrazine is found to remove the ligands from the surface of the NCs, improving conductivity to enhance charge transport. Four point probe and Hall measurement studies showed comparatively low resistivity of the NC film (<100 Ω-cm), high carrier concentration (~10^{19} cm^{-3}) and low mobility (<1 cm^2/V.s). Because of the high carrier concentration and low mobility, these NC films could not be utilized as an absorber layer in high-performance thin film solar cells. However, the FeS_2 NC films' high free carrier concentration and iron pyrite's large work function (~5.45 eV) which compares favorably with that of Au,[12, 13] support excellent performance as a low-barrier back contact for CdS/CdTe superstrate solar cells.

B. FeS_2 as a back contact of CdS/CdTe solar cells

Representative current density vs. voltage (J-V) characteristics for sputtered CdTe devices prepared with different back contacts are shown in Fig. 2 and their parameters are shown in Table 1. Back contacts studied here include: 30 nm Au only; 3 nm Cu with 30 nm Au;,and ~1μm FeS_2 with 30 nm Au. In J-V measurements, solid lines represent the light response and dashed lines represent the dark response of the devices. Despite a good J_{sc} the Au-only device shows a low V_{oc} (0.65 V) and low efficiency (7.7%). Because of the high electron affinity for CdTe, -4.5 eV from the vacuum level [14], a high work function metal is required to form a barrier-free contact to p-type CdTe. Therefore, when forming a metallic back contact to CdTe, a barrier typically forms which inhibits hole transport at the back contact and reduces both V_{oc} and FF. This problem is largely alleviated by depositing ~3 nm Cu onto CdTe and annealing the film at 150°C for ~40 minutes. Copper helps to reduce the effective barrier by increasing the doping level of CdTe through inter-diffusion and formation of a thin $Cu_{2-x}Te$ layer, and enabling efficient through-barrier tunneling.[15] This Cu-Au two step back contact improved V_{oc} from 0.65 V to 0.77 V, and efficiency improved from 7.7% to 10.0% as shown by the blue curve in Fig. 2 and the performance parameters in Table 1.

When 3 nm Cu was replaced by a ~1.5 μm thick FeS_2 NC layer deposited at room temperature, followed by 30 nm of Au, performance of the device was nearly identical to the Cu/Au case represented by black curve in Fig. 2. In this case, we measured the V_{oc} to be 0.77 V, a J_{sc} of 21.4 mA cm^{-2} and 9.6% efficiency. In contrast to the Cu/Au contact, the

FeS_2/Au contact was not heated. A relatively thick layer of FeS_2 was deposited onto CdTe layer to prevent Au from reaching the CdTe layer via filling of pin holes within the NC layer.

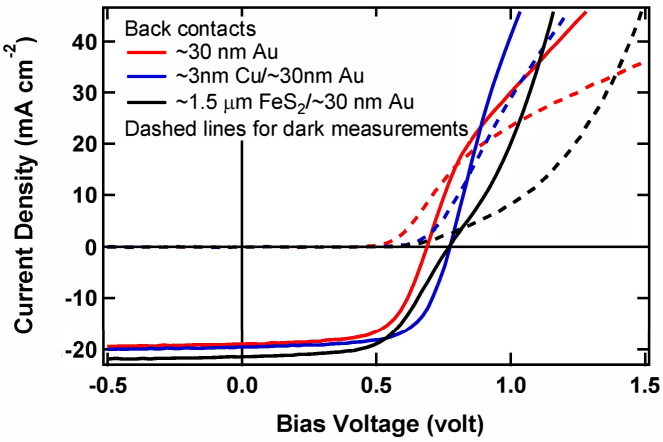

Fig. 2. Current density vs bias voltage measurements of CdS/CdTe device with Au, Cu/Au, and FeS_2/Au back contacts obtained under simulated AM1.5G solar spectrum.

Table 1. Sputtered solar cell parameters for three different back contact types.

Back contact	V_{oc} (V)	J_{sc} (mA cm^{-2})	Fill Factor (%)	Efficiency (%)	Series resistance (Ω cm^2)
Au	0.648	18.6	64.3	7.7	6.1
Cu/Au	0.774	19.5	66.1	10.0	4.9
FeS_2/Au	0.771	21.4	58.3	9.6	12.6

To optimize the FeS_2 NC thickness as a back contact, we used high efficiency CdTe solar cells for which the CdTe was deposited by CSS. An optimized CSS CdTe device fabricated by the UT team with an application of elemental Cu/Au back contacts has reached 15.5% under AM1.5G simulated solar radiation. [16] In our application, we have used a CdTe device stack showing an optimal Cu/Au standard back contact efficiency of 14.3%. We fabricated and measured Cu-free FeS_2 back contact with FeS_2 thickness varying from 0.35 to 1.4μm and obtained optimized efficiency of 12.5%, V_{oc} = 0.81V, J_{sc} = 23.0 mA cm^{-2} and FF = 67%. We found an optimal FeS_2 film thickness of ~750 nm; the thinner ~350 nm FeS_2 film likely exposes CdTe directly to Au through pinholes, reducing V_{oc} and efficiency. The thickest FeS_2 film appears to show an increased effective series resistance and a larger inflection indicative of a slightly increased barrier at the back contact.

C. *Temperature dependent study of FeS_2 NC*

The temperature dependence of the conductivity for two different thick FeS_2 NC films is shown in Fig. 3. Conductivity decreases exponentially from 300 to 80 K which indicates the semiconducting nature of the FeS_2 NC films. In general, the conductivity of an insulating disordered system, such as surfactant-capped NC films, decreases with decreasing temperature and can typically be described by Eq. (1) [17]

$$\sigma = \sigma_O Exp\left(\frac{-T_O}{T}\right)^x \quad (1)$$

where, σ and σ_o are electrical conductivities at temperature T and 0 K respectively [18]. The temperature exponent x depends on the transport mechanism. When x = 1, the conductivity is due to the nearest neighbor hopping (NNH), where the conductivity is primarily from tunneling between neighboring NCs. Similarly, x = 0.5 corresponds to Efros-Shklovskii variable-range hopping (ES-VRH) model[19], x = 0.25 and x = 0.33 correspond to Mott variable- range (M-VRH) models in three and two dimensional transport respectively[20, 21]. These hopping mechanisms arise in situations where the transport of carriers is carried primarily by 'co-tunneling' events between the neighboring NCs.[22]

Fig. 3 shows a logarithmic conductivity data for NC films of thicknesses t = 486 nm and t = 850 nm; our preliminary analysis indicates that at low temperature a value for x in the range of ~0.25 to ~0.35 gives a good fit, with a significant uncertainty remaining. Additional studies are underway to improve precision.

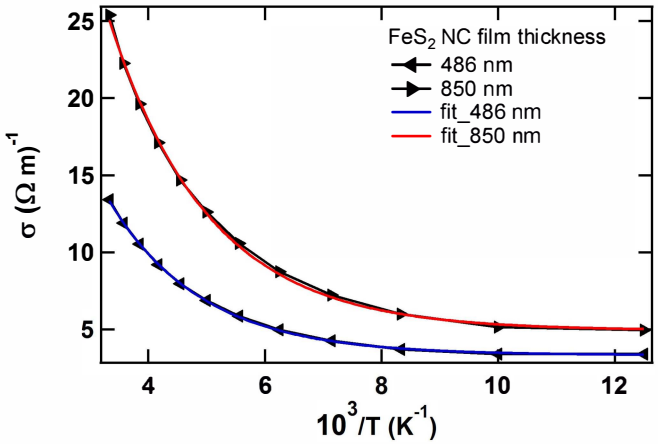

Fig. 3. (a) Temperature dependence of conductivity of FeS_2 films for 486 nm (blue curve) and 850 nm (red curve) thicknesses.

Based on the literature study, we find an exponent of 0.25 [23] and 0.5 [24] for temperature dependent conductivity study of PbSe and CdSe NCs respectively. Kang et al. also found that a range of exponents, 0.5, 0.33 and 0.25, fit their data for the temperature dependent study of PbSe NC thin films.[20] An exponent of x = 1 can be used to fit the near room temperature range of Fig. 3. This indicates that at high temperature the system may show Arrhenius behavior. As the temperature decreases, VRH appears dominant.

D. *Temperature dependent JV characteristics of CdTe solar cells using different back contacts*

Fig. 4 shows temperature dependent JV characteristics of CdS/CdTe solar cells for three different types of back contacts. These measurements were done under excitation from a Kodak Projector light source for which it is very difficult to establish and control an AM1.5G equivalent illumination at the photovoltaic devices. As such, the current densities reported here result from slightly higher or lower illumination intensity and should not be considered as device characteristics. We are reporting these results for qualitative comparison of the temperature-dependent photocurrent and photovoltage. Fig. 4a shows JV curves when the standard Cu/Au was used as the back contact while Fig. 4b and Fig. 4c utilize as-synthesized and hydrazine-treated FeS_2 NCs respectively in place of the Cu layer. At room temperature, the Cu/Au back contact device shows very nice diode behavior but the back barrier influence becomes evident at decreasing temperature. The devices having untreated-FeS_2/Au as back contact were influenced significantly by temperature (Fig. 4b) whereas influences in the performance can also be seen in hydrazine treated-FeS_2/Au back contact devices Fig. 4c with good diode behavior at room temperature and a clear S-kink behavior arising at low temperatures.

It is known that semiconductors have temperature dependent band gap through the temperature dependence of the structural parameters.[25, 26] Typically semiconductors show an increasing band gap energy as temperature is reduced.[27] The temperature dependent band gap was studied in the past for both single crystalline and thin film CdTe and was found to decrease of band gap with increase of temperature.[28-31] Using Manoogian-Wooley (M-W) equation [32] with the coefficients obtained by Fonthal et al.[31], band gap of the CdTe was calculated at 80K and 300K, the extremes of our temperature range, and was obtained to be 1.59 eV and 1.51 eV respectively. The change in band gap energy is 0.08 eV and the expected decrease in J_{sc} when temperature drops from 300 to 80 K is ~2.6 mA cm^{-2}. This expected change in J_{sc} is calculated assuming that all the photons above the given band gap energy contribute efficiently to the photocurrent. Due to a decrease in the intrinsic carrier concentration and the concomitant reduction in reverse saturation current, V_{oc} is expected to increase at decreasing temperatures following Eq (2).

$$V_{OC} = \frac{Ak_BT}{q}\ln\left(\frac{J_{sc}}{J_O}+1\right) \qquad (2)$$

,where A is the diode quality factor, and J_o is the reverse saturation current density. Fig. 4a shows behavior in accord with these typical behaviors, although it is clear that a rapidly-decreasing FF exhibits substantial influence on the behavior of

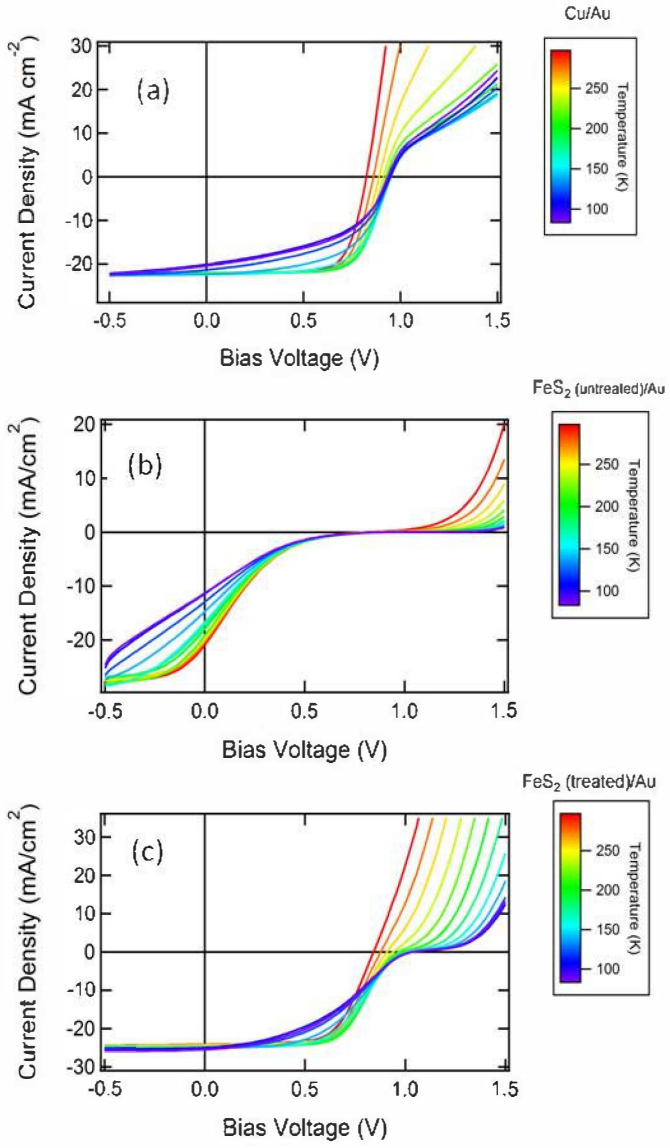

Fig. 4. Temperature dependent JV characteristics in three different back contacts: (a) Cu/Au, (b) FeS_2 (untreated)/Au and (c) FeS_2 (treated)/Au.

J_{sc}. When Cu is replaced by untreated NC-FeS_2, J_{sc} is more strongly affected at low temperature as shown in Fig. 4b. Poor mobility expected within the untreated NC-FeS_2 contact layer yields complicated behavior, with a poorly-defined V_{oc} influenced strongly both by the nature of the effective barrier associated with the insulating ligands left intact between neighboring FeS_2 NCs, and by the resulting S-kink J-V behavior. In a typical semiconductor materials, reduced lattice scattering tends to increase the mobility with decreasing temperature, while the charge carriers' lower average thermal velocity leads to an increased impurity scattering, which decreases mobility.

As shown in Fig. 4a, J_{sc} has decreased by 2 mA cm^{-2} when the temperature is decreased from 300 K to 80 K, which is close to the expected decrease in J_{sc} (2.6 mA cm^{-2}). This

decrease in J_{sc} may also be due to the increase in series resistance and reduction in shunt resistance. In Fig. 4b, the decrease in J_{sc} is 10 mA cm^{-2}, which is higher than expected value in CdS/CdTe solar cell. This decrease in J_{sc} likely arises from significantly reduced mobility in the untreated FeS_2 NC film. When the back contact consists of hydrazine-treated FeS_2/Au, Fig. 4c, J_{sc} is rather increased by ~1 mA cm^{-2} when the temperature is decreased from 300K to 80K. Although additional testing of this behavior is merited, these initial results indicate that the hydrazine treated FeS_2 NC back contact maintains the constant J_{sc} despite the expected decrease in reverse saturation current.

As shown in Fig. 4a, at low temperature, the forward current is severely limited by the back-contact-barrier developed at the CdTe/Cu/Au interface. The band gap is increased by 0.08 eV at low temperature but without additional experiments, we are unable to determine whether there is a change in electron affinity or work function of the CdTe due to this band gap change. For n-InP, when the temperature was increased from 0 to 400 K, band gap was decreased by 0.2 eV and electron affinity was also increased by the same amount, with similar behavior observed for GaAs.[33] In other words, as the bandgap energy decreases at higher temperature, the valence band edge remains approximately fixed relative to the vacuum level, while the conduction band edge moves away from the vacuum level. However, our experimental results for CdTe/Cu/Au suggest that the valence band edge may have moved to more negative values (away from the vacuum level). If so, then at low temperature the increase in the CdTe band gap energy would increase the barrier height for hole transport to the Au layer. In addition, the Cu-doped p+ layer's free carrier concentration will decrease and therefore widen the barrier and inhibit tunneling. In comparison with the CdTe/Cu/Au device, which shows "roll-over" of the current at forward bias, the CdTe/FeS_2/Au device shows increasing S-Kink behavior as temperature decreases (Fig. 4c).

As mentioned above, when the back contact is treated-FeS_2/Au, J_{sc} remains approximately constant with temperature (Fig. 4c), and V_{oc} depends principally on J_o with significant influence from the S-kink shaping near J = 0 mA. The reverse saturation current is due to the recombination in the quasi-neutral region of the device and is itself highly sensitive to temperature changes, increasing exponentially with increasing temperature.

V. CONCLUSION

Even though the FeS_2 NCs we synthesized here were phase pure and highly crystalline, their applications are limited to the copper free back contact of CdTe thin film solar cells. This work presents the first illustration of using FeS_2 NC as a low barrier electrical contact to thin film solar cells without post surface modification. The temperature dependent study of the hydrazine treated FeS_2 NC films shows that the transport of charge carriers is governed by variable range hopping – most likely either or both ES-VRH and M-VRH conduction mechanisms. The temperature dependent study of current voltage characteristics of CdS/CdTe solar cells with FeS_2/Au back contact reveals near-ohmic contact between FeS_2/Au interfaces. We are in the preliminary stage of this study where we have begun to use FeS_2 as a back contact of CdTe solar cells. Our future work will focus to optimize FeS_2 NC thin films to optimize the performance as a copper free back contact for CdS/CdTe thin film solar cells. This work represents an important and unexpected advance in the application of FeS_2 within thin film solar cells.

ACKNOWLEDGEMENT

KPB, YY, NRP, and RJE were supported by the National Science Foundation's Sustainable Energy Pathways Program under grant CHE-1230246; PK and RWC were supported by the DOE/NSF F-PACE Program (Contract DE-EE0005405). RRK and MJH were supported by the Department of Energy under Award Number DE-SC0006349 and by faculty start-up funds from the University of Toledo. KPB, PJR, TK and RJE also gratefully acknowledge support from Air Force Research Laboratory under contracts FA9453-08-C-0172 and FA9453-11-C-0253.

REFERENCES

[1] A. Ennaoui, *et al.*, "Iron disulfide for solar energy conversion," *Solar Energy Materials and Solar Cells,* vol. 29, pp. 289-370, 5// 1993.

[2] Y. Bi, *et al.*, "Air Stable, Photosensitive, Phase Pure Iron Pyrite Nanocrystal Thin Films for Photovoltaic Application," *Nano Letters,* vol. 11, pp. 4953-4957, 2011/11/09 2011.

[3] J. Puthussery, *et al.*, "Colloidal Iron Pyrite (FeS2) Nanocrystal Inks for Thin-Film Photovoltaics," *Journal of the American Chemical Society,* vol. 133, pp. 716-719, 2011/02/02 2010.

[4] A. Kirkeminde, *et al.*, "All inorganic iron pyrite nano-heterojunction solar cells," *Nanoscale,* vol. 4, pp. 7649-7654, 2012.

[5] T. J. Berniard, *et al.*, "Effects of Cu at the device junction on the properties of CdTe⁄ CdS photovoltaic cells," *Journal of Vacuum Science & Technology B,* vol. 22, pp. 2423-2428, 2004.

[6] S. H. Demtsu, *et al.*, "Cu-related recombination in CdS/CdTe solar cells," *Thin Solid Films,* vol. 516, pp. 2251-2254, 2/29/ 2008.

[7] K. V. Krishna and V. Dutta, "Effect of in situCdCl2 treatment on spray deposited CdTe⁄ CdS heterostructure," *Journal of Applied Physics,* vol. 96, pp. 3962-3971, 2004.

[8] P. Lazić, *et al.*, "Low intensity conduction states in FeS2: implications for absorption, open-circuit voltage and surface recombination," *Journal of Physics: Condensed Matter,* vol. 25, p. 465801, 2013.

[9] T. E. Webber, "Synthesis of Iron Pyrite and Tin (VI) Sulfide Nanoparticles for Potential Application in Solar Cells."
[10] S. N. White, "Laser Raman spectroscopy as a technique for identification of seafloor hydrothermal and cold seep minerals," *Chemical Geology,* vol. 259, pp. 240-252, 2009.
[11] M. Eghbalnia, "Electrochemical and Raman investigation of pyrite and chalcopyrite oxidation," 2012.
[12] Y. A. Liu, "Physical cleaning of coal: present and developing methods," Marcel Dekker, Inc., New York, NY1982.
[13] S. Trigwell, *et al.*, "Tribocharging in electrostatic beneficiation of coal: Effects of surface composition on work function as measured by x-ray photoelectron spectroscopy and ultraviolet photoelectron spectroscopy in air," *Journal of Vacuum Science & Technology A,* vol. 19, pp. 1454-1459, 2001.
[14] K. Durose, *et al.*, "Materials aspects of CdTe/CdS solar cells," *Journal of Crystal Growth,* vol. 197, pp. 733-742, 2/15/ 1999.
[15] C. R. Corwine, *et al.*, "Copper inclusion and migration from the back contact in CdTe solar cells," *Solar Energy Materials and Solar Cells,* vol. 82, pp. 481-489, 5/30/ 2004.
[16] N. R. Paudel and Y. Yan, "Fabrication and characterization of high-efficiency CdTe-based thin-film solar cells on commercial SnO2:F-coated soda-lime glass substrates," *Thin Solid Films,* vol. 549, pp. 30-35, 2013.
[17] S. O. Kasap, *Principles of electronic materials and devices* vol. 3: McGraw-Hill New York, NY, 2006.
[18] B. I. Shklovskii and A. L. Efros, "Electronic properties of doped semiconductors," *Moscow Izdatel Nauka,* vol. 1, 1979.
[19] A. Efros and B. Shklovskii, "Coulomb gap and low temperature conductivity of disordered systems," *Journal of Physics C: Solid State Physics,* vol. 8, p. L49, 1975.
[20] M. S. Kang, *et al.*, "Size-and temperature-dependent charge transport in PbSe nanocrystal thin films," *Nano Letters,* vol. 11, pp. 3887-3892, 2011.
[21] N. Mott, "Conduction in non-crystalline materials: III. Localized states in a pseudogap and near extremities of conduction and valence bands," *Philosophical Magazine,* vol. 19, pp. 835-852, 1969.
[22] T. Chen, *et al.*, "Hopping conduction in assemblies of hydrosilylated silicon nanocrystals," *arXiv preprint arXiv:1401.6713,* 2014.
[23] D. V. Talapin and C. B. Murray, "PbSe Nanocrystal Solids for n- and p-Channel Thin Film Field-Effect Transistors," *Science,* vol. 310, pp. 86-89, October 7, 2005 2005.
[24] D. Yu, *et al.*, "Variable Range Hopping Conduction in Semiconductor Nanocrystal Solids," *Physical Review Letters,* vol. 92, p. 216802, 05/25/ 2004.
[25] N. Peyghambarian, *et al.*, *Introduction to semiconductor optics*: Prentice-Hall, Inc., 1994.
[26] Y. Varshni, "Temperature dependence of the energy gap in semiconductors," *Physica,* vol. 34, pp. 149-154, 1967.
[27] B. Van Zeghbroeck, "Principles of semiconductor devices," *Colorado University,* 2004.
[28] G. Mahan, "Temperature dependence of the band gap in CdTe," *Journal of Physics and Chemistry of Solids,* vol. 26, pp. 751-756, 1965.
[29] D. Poelman and J. Vennik, "The temperature dependence of the optical properties of thin CdTe films," *Journal of Physics D: Applied Physics,* vol. 21, p. 1004, 1988.
[30] X. Mathew, "Band gap of CdTe thin films—The dependence on temperature," *Journal of materials science letters,* vol. 21, pp. 529-531, 2002.
[31] G. Fonthal, *et al.*, "Temperature dependence of the band gap energy of crystalline CdTe," *Journal of Physics and Chemistry of Solids,* vol. 61, pp. 579-583, 4// 2000.
[32] A. Manoogian and J. Woolley, "Temperature dependence of the energy gap in semiconductors," *Canadian journal of physics,* vol. 62, pp. 285-287, 1984.
[33] W. Mönch and N. J. Dinardo, "Semiconductor surfaces and interfaces," *Physics Today,* vol. 47, pp. 66-67, 2008.